
PHYSICS-BASED APPROXIMATION AND PREDICTION OF SPEEDLINES IN COMPRESSOR PERFORMANCE MAPS

THK-AI RESEARCH REPORT 1/2026

Abdul-Malik Akiev

TH Köln, Germany

abdul-malik.akiev@smail.th-koeln.de

Alexander Schirger

TH Köln, Germany

alexander.schirger@smail.th-koeln.de

Alexander Hinterleitner 

THK-AI Research Cluster, TH Köln

alexander.hinterleitner@th-koeln.de

Danyal Ergür

TH Köln, Germany

danyal_arda.erguer@smail.th-koeln.de

Matthias Müller

Everllence SE, Turbolader Entwicklung

matthias.mueller.c@everllence.com

Thomas Bartz-Beielstein 

THK-AI Research Cluster, TH Köln

thomas.bartz-beielstein@th-koeln.de

March 13, 2026

ABSTRACT

Speedlines in compressor performance maps (CPMs) are critical for understanding and predicting compressor behavior under various operating conditions. We investigate a physics-based method for reconstructing compressor performance maps from sparse measurements by fitting each speedline with a superellipse and encoding it as a compact, interpretable vector (surge, choke, curvature, and shape parameters). Building on the formulation of Llamas et al., we develop a robust two-stage fitting pipeline that couples global search with local refinement. The approach is validated on industrial data-sets for different turbocharger types. We discuss prediction quality for inter- and extrapolation, metric sensitivities and outline opportunities for physics-informed constraints, alternative function families, and hybrid physics–ML mappings to improve boundary behavior and, ultimately, enable full CPM reconstruction from limited data.

1 Introduction

Compressor performance maps (CPMs) play a crucial role in the design, evaluation, and control of turbocharged engines and gas turbines. These maps characterize the relationship between the corrected mass flow, the pressure ratio, and the rotational speed of a compressor. However, generating accurate CPMs requires extensive measurements on test benches, which are time-consuming, expensive, and often limited to discrete operating points and speedlines. Therefore, there is a strong demand for reliable algorithms that can reconstruct or predict miss-

ing speedlines or even entire CPMs from sparse measurements (Shen et al., 2019). Recent advances in machine learning have shown promising results in approximating CPMs using data-driven methods such as recurrent neural networks (RNNs) (Schulz et al., 2025), which model the structure of speedlines as sequences and learn their behavior from a large number of maps. While these approaches achieve high accuracy in interpolation and extrapolation tasks, they require significant amounts of training data and often lack physical interpretability.

In this report, we present a slightly modified physics-based approach to CPM reconstruction and prediction

based on a geometric fitting procedure. Specifically, we approximate each speedline using a *superellipse*, as proposed by Llamas and Eriksson (2019), and represent each fitted speedline via a compact β -vector containing physically meaningful parameters. Based on this representation, we interpolate and extrapolate β -vectors to predict unknown speedlines at other rotational speeds. Our approach offers three key advantages: a low-dimensional, interpretable parameterization of speedlines, excellent interpolation capability particularly in mid-speed regions, and minimal data requirements, relying on only a few known speedlines.

This paper is structured as follows: Section 2 describes the background and motivation for this work, including the industrial context and related research. Section 3 details our method, including the superellipse fitting procedure, the prediction strategy using β -vectors, and the evaluation framework. Section 4 presents the experiments to assess interpolation and extrapolation performance. Section 5 discusses the related results in detail. Finally, Section 6 discusses the implications of our findings, limitations of the current approach, and potential directions for future research.

2 Background and Motivation

This project was conducted as part of the so-called “Teamprojekt” module within the Bachelor’s program in Electrical Engineering—Automation Technology at the THK-AI Research Cluster at TH Köln (<https://thk-ai.de>). The module encourages students to independently design and implement a technical-scientific project in collaboration with an external industrial partner. The project is embedded in a joint research initiative with Everllence (formerly known as MAN Energy Solutions), a company specializing in high-performance turbomachinery. As part of this collaboration, Everllence has provided access to an internal dataset consisting of approximately 15 CPMs, measured from two different types of turbochargers. These real-world datasets serve as the basis for the prediction and model validations conducted in this work.

Within this research initiative, a second team is developing a machine learning-based approach using recurrent neural networks (RNNs) to model CPMs. Their work focuses on exploiting sequential structures within speedlines to interpolate and extrapolate operating data using data-driven techniques. Their results are documented in a separate scientific paper forming the core of the machine-learning branch of this study (Schulz et al., 2025).

In contrast to the machine-learning approach, our team investigates a physics-based alternative approach. Our method models each speedline using a superellipse parameterization, inspired by the work of Leufvén and Eriksson (2013) and further extended by Llamas and Eriksson (2017). We encode each speedline into a compact β -vector consisting of interpretable parameters (e.g.,

surge, choke, curvature) and then interpolate or extrapolate between these vectors to predict unknown speedlines.

The overarching motivation of this work is exploratory in nature. We aim to assess how well a physically structured approximation method can reconstruct compressor maps when provided with limited measurement data. Although full CPM prediction is not the primary goal, the long-term aspiration is to enable robust, low-data reconstructions of entire performance maps using physically meaningful abstractions. By aligning our evaluation criteria with those of the RNN-based approach, we seek to enable a fair and quantitative comparison between physics-informed and machine learning methods in the domain of turbomachinery modeling.

3 Method

3.1 Superellipse Model

Our implementation builds upon the superellipse model proposed by Llamas and Eriksson (2019), extending it with robust optimization strategies. The model approximates each speedline using a parameterized superellipse curve, characterized by a β -vector containing physically meaningful parameters such as surge point, choke point, and shape parameters. The superellipse formulation following Llamas and Eriksson (2019) is given by:

$$\left(\frac{\dot{m} - \dot{m}_{zs}}{\dot{m}_{ch} - \dot{m}_{zs}} \right)^{\text{CUR}} + \left(\frac{\Pi - \Pi_{zs}}{\Pi_{ch} - \Pi_{zs}} \right)^{\text{CUR}} = 1, \quad (1)$$

where \dot{m}_{zs} and Π_{zs} represent the surge point, \dot{m}_{ch} and Π_{ch} the choke point, and CUR the curvature parameter that controls the shape of the speedline. These parameters form the β -vector $\beta = [\dot{m}_{zs}, \Pi_{zs}, \dot{m}_{ch}, \Pi_{ch}, \text{CUR}]^T$ (Shen et al., 2019).

The key innovation in our approach lies in the optimization procedure. Instead of relying on simple initialization with heuristics and local optimization, we implement a multi-stage fitting process. The optimization procedure consists of three main stages. First, the global parameter initialization employs either Particle Swarm Optimization (PSO) with configurable swarm size (default: 100 particles, 50 iterations) or Differential Evolution (DE) with population size 15 and up to 1,000 iterations (Storn and Price, 1997; Kennedy and Eberhart, 1995). Both methods thoroughly explore the parameter space to avoid local minima. The second stage implements a local optimization pipeline using L-BFGS-B as the primary solver with a maximum of 5,000 iterations, automatically falling back to Nelder-Mead if L-BFGS-B fails (Nelder and Mead, 1965; Broyden, 1970). This is followed by comprehensive bounds validation to ensure solution validity.

For performance assessment, we employ multiple error metrics. While the above description outlines the default configuration, all parameters in both the fitting process

and later prediction can be customized through a configuration interface. This includes swarm sizes, iteration counts, solver choices, error metrics, etc. The described settings represent our defaults based on the first experiments, but users can adjust these parameters to suit specific requirements or performance needs.

3.2 Prediction Using β Vectors

After fitting individual speedlines to obtain β -vectors, we use polynomial interpolation to predict unknown speedlines. The process is identical regardless of whether the target speed lies within the known range (interpolation) or outside it (extrapolation). The prediction process follows a systematic approach with three key components. The hold-out strategy begins by removing the target speedline from the dataset, followed by fitting all remaining speedlines to obtain their β -vectors, which are then used to predict the held-out speedline. For polynomial fitting, we employ 4th-degree polynomials fitted independently to each β parameter, with optional speed normalization to the $[0,1]$ range for numerical stability. Physical constraints are enforced throughout the process, such as maintaining curvature ≥ 2 and ensuring non-negative values. The final parameter prediction stage involves evaluating these polynomials at the target speed to obtain the predicted β -vector, followed by applying post-processing constraints to ensure physical validity of the results.

Similar to the fitting process, all prediction parameters can be customized through a configuration class. This includes the polynomial degree, normalization settings, parameter constraints and the evaluation mode (pressure-based or mass flow-based). The described settings represent our defaults based on the first experiments, but users can adjust these parameters according to their specific needs. Our approach can be seen as an extension of the approach by Shen et al. (2019), who use a polynomial degree of 2 and a normalization to the $[0,1]$ range.

3.3 Evaluation and Error Assessment

After predicting a β -vector for the target speedline, we evaluate the prediction quality using multiple error metrics. Our evaluation framework encompasses three comprehensive aspects. For prediction evaluation, we implement two distinct modes: a pressure-based approach comparing predicted pressure ratios π at given mass flows \dot{m} , and a mass flow-based approach comparing predicted mass flows \dot{m} at given pressure ratios π . Both modes utilize actual measurement points from the held-out speedline for comparison. The assessment employs multiple error metrics.

For model assessment we employ RMSE (absolute units), MAPE (relative %), the residual standard deviation (solver consistency), and the orthogonal distance

$$\text{ortho} = \sum_{i=1}^N \left\| \mathbf{x}_i^{\text{true}} - \mathbf{x}_i^{\text{pred}} \right\|^2$$

in the (\dot{m}, π) space. Because each metric has its own scale and interpretation, direct numerical aggregation or comparison is inappropriate (Hyndman and Koehler, 2006). RMSE accentuates large outliers, MAPE scales each error by its true value (and fails when $y \approx 0$), the residual SD captures run-to-run stability, whereas ortho measures the geometric fidelity of the entire speed-line. We therefore report all metrics separately and consider a solver successful only when it achieves simultaneously low means and dispersions in at least two metrics. Our statistical-analysis methodology ensures robustness by calculating both mean errors and standard deviations, carefully handling numerical edge cases such as division by zero and invalid predictions, and providing comprehensive error statistics for thorough model comparison.

4 Experiments

4.1 Dataset and Preprocessing

Our experiments are conducted on a simulated dataset, a public benchmark dataset and a comprehensive dataset provided by Everllence, consisting of 15 compressor performance maps from two different turbocharger types. Each map contains multiple speedlines with varying numbers of measurement points across different operating conditions. The preprocessing involves two main steps: normalization of mass flow and pressure ratio values, and consistent speedline identification together with grouping to ensure data quality.

4.2 Fitting Optimization Study

The first experimental phase focused on establishing the most robust fitting procedure for individual speedlines (no prediction). Our benchmark study evaluated three key aspects. For model implementations, we compared the LlamasEllipse implementation following Llamas and Eriksson (2019) with the DirectEllipse approach based on direct least squares fitting (Fitzgibbon et al., 1999). The DirectEllipse method transforms the geometric problem into a generalized eigenvalue system:

$$\mathbf{S}\mathbf{a} = \lambda\mathbf{C}\mathbf{a},$$

where $\mathbf{a} = [a, b, c, d, e, f]^T$ represents the coefficients of the general conic equation

$$ax^2 + bxy + cy^2 + dx + ey + f = 0,$$

and \mathbf{S} and \mathbf{C} are scatter and constraint matrices ensuring the elliptical shape.

We investigated three optimization strategies: a baseline approach using direct L-BFGS-B optimization, a PSO-enhanced method, and a DE-enhanced approach. For performance evaluation, we employed the error metrics discussed in Section 3.3. Each configuration was evaluated using simulated data to establish baseline performance and identify the most robust parameter estimation approach.

4.3 Prediction Method Validation

The second phase validated our prediction methodology using a public benchmark dataset (tca_88): Our validation methodology comprised three key aspects. The hold-out Strategy involved systematic testing of different speedline hold-out positions, comprehensive analysis of interpolation versus extrapolation performance, and thorough validation of polynomial degree selection. For parameter constraints, we focused on implementing physical bounds for β -vectors, validating surge/choke point predictions, and assessing the stability of the curvature parameter. The numerical stability analysis encompassed testing of speed normalization effects, evaluating polynomial fitting robustness, and developing comprehensive prediction confidence metrics.

4.4 Industrial Dataset Evaluation

The final experimental phase applied our optimized approach to the complete Everllence dataset: The evaluation consisted of two main components. Our cross-validation approach implemented leave-one-out validation for each speedline, coupled with detailed statistical analysis of prediction errors and a thorough comparison of interpolation versus extrapolation accuracy. The performance assessment phase evaluated the method across two different turbocharger types, each with distinct characteristics in terms of speed ranges, number of speedlines, and measurement point density. This comprehensive evaluation allowed us to quantify prediction reliability across diverse operational conditions.

5 Results

5.1 Fitting Optimization Study

Our comprehensive benchmark of different fitting strategies revealed several key insights about the optimization of the superellipse parameters (Eq. 1). The analysis focused on comparing different combinations of initialization strategies, solvers, and error metrics.

The LlamasEllipse model consistently outperformed the DirectEllipse approach across multiple metrics. The model achieved lower values across all error metrics, though this alone does not guarantee better performance. More importantly, it demonstrated superior performance in capturing the overall shape of the speedline, which is crucial for accurate compressor modeling. Figure 1 compares the performance of the LlamasEllipse and DirectEllipse models using the best performing configuration on the tca88 dataset, demonstrating the superior performance of the LlamasEllipse model across all error metrics.

The orthogonal distance (ortho) metric emerged as the most suitable objective function. It excels in several aspects: it provides better geometric accuracy of fitted curves, shows enhanced robustness against outliers com-

pared to MSE/RMSE/MAPE, and maintains consistent performance across different speed ranges. Most importantly, it serves as an intuitive geometric metric that is both easy to interpret and numerically stable, avoiding NaN or infinite values in calculations.

The combination of DE with Nelder-Mead as solver and ortho as error metric proved to be the most robust on the LlamasEllipse model. Importantly the initial guess optimization proved crucial, drastically enhancing final optimization performance and reducing maximum error by 67% compared to direct optimization. DE optimization of initial parameters slightly outperformed PSO, achieving a mean ortho improvement of 84% compared to 81%. Additionally, Nelder-Mead demonstrated superior convergence characteristics compared to L-BFGS-B, particularly for challenging speedline configurations.

Based on these results, we selected the LlamasEllipse model with DE initialization (population size 15, 1000 iterations), Nelder-Mead as solver, and ortho as the error metric for all subsequent experiments. This configuration provided the best balance between fitting accuracy and numerical stability. Figure 2 shows a detailed comparison of the three optimization approaches (no pre-optimization, PSO, and DE) in terms of RMSE and maximum error on the tca88 dataset. The results show that the pre-optimization provides better results compared to the direct optimization approach.

5.2 Interpolation Within CPMs

The interpolation results for the tca88 dataset demonstrate the effectiveness of our prediction approach, as shown in Figure 3. The left plot illustrates the predicted speedlines overlaid with the actual measurements, while the right plot shows the evolution of the β coefficients across different speeds, providing insight into the interpolation behavior.

A notable observation from our experiments is that MAPE proves to be an unreliable metric for assessing prediction quality in our context. For instance, at 400 m/s (Index 3), we observe a MAPE of $161.23\% \pm 356.93\%$, which suggests poor performance, yet the visual fit is reasonable. This discrepancy arises because MAPE is highly sensitive to small absolute differences when the reference values are close to zero, which is common in our normalized data. Instead, the orthogonal distance metric ortho provides more meaningful insights into prediction quality. Most predictions show excellent ortho values below 0.01, indicating high accuracy. The best results were achieved at 475 m/s (Index 5) with $\text{ortho} = 0.0013 \pm 0.0027$, followed by 450 m/s (Index 4) with $\text{ortho} = 0.0031 \pm 0.0057$, and 525 m/s (Index 7) with $\text{ortho} = 0.0059 \pm 0.0070$.

An interesting case is the prediction at 350 m/s (Index 2), which shows a relatively high ortho value of 2.0656 ± 4.0088 despite visually excellent fit quality, same applies for the speed 500 m/s (Index 6). This apparent contra-

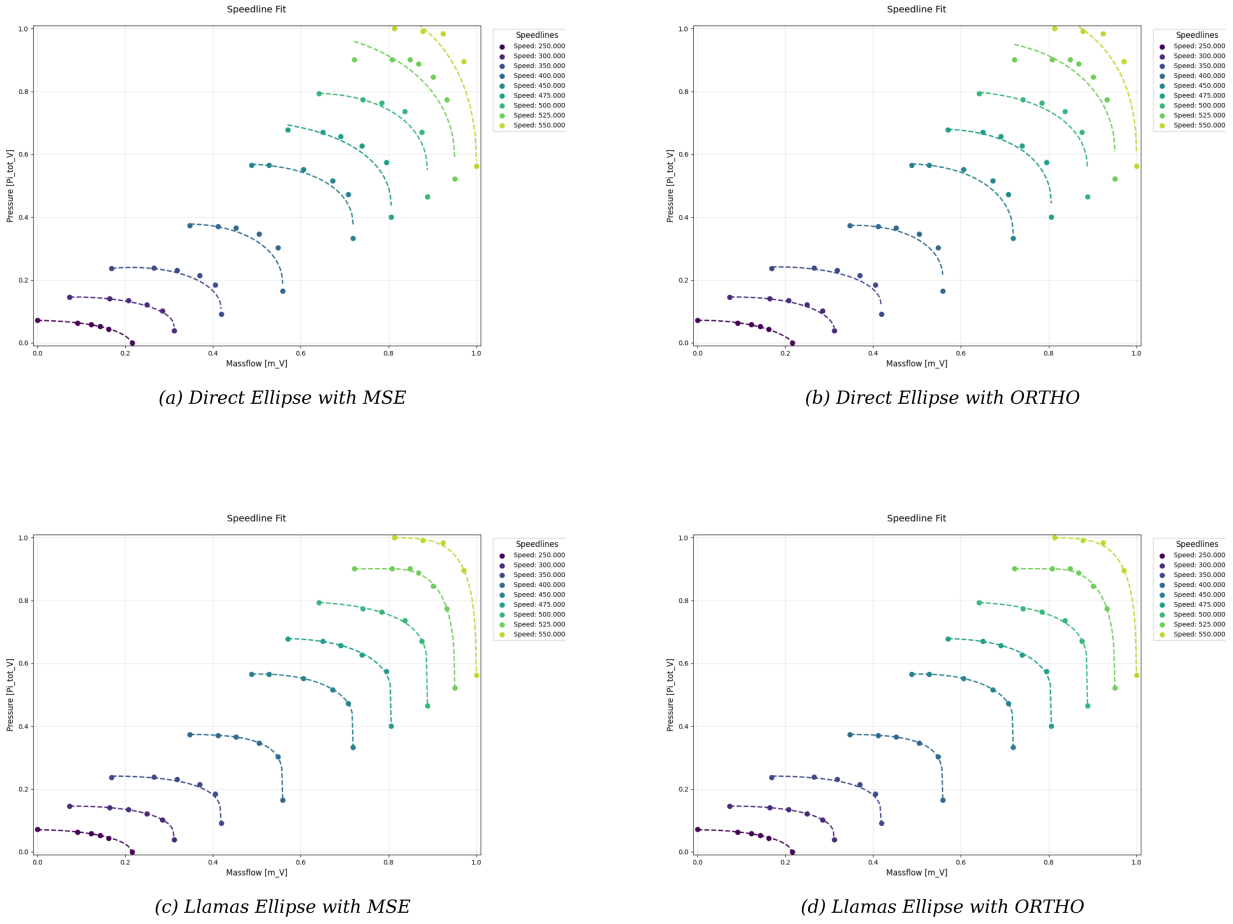


Figure 1: Comparison of DirectEllipse and LlamasEllipse models using the best performing configuration on the tca88 dataset

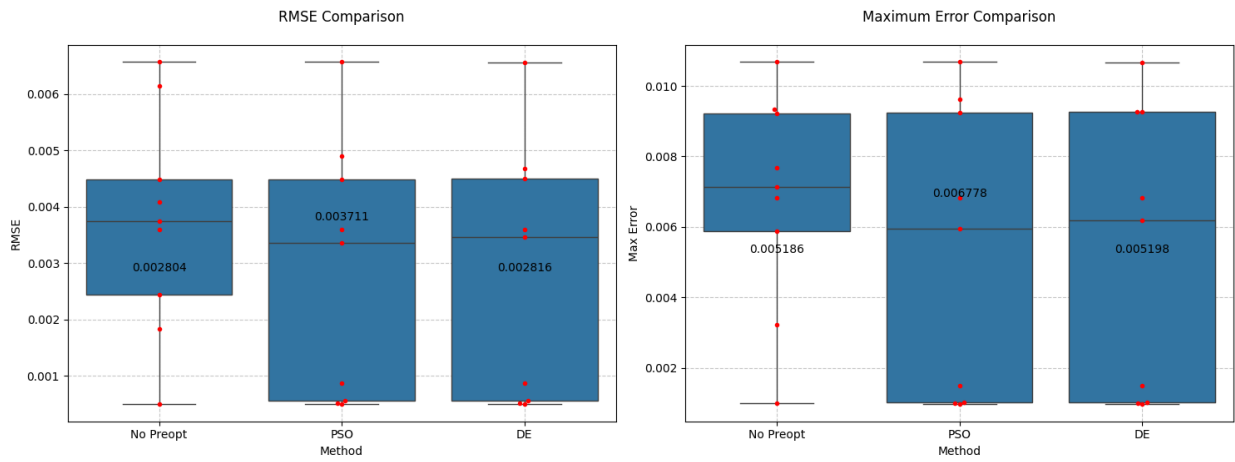


Figure 2: Comparison of optimization strategies. The boxplots show the distribution of RMSE and maximum error across all speedlines in the tca88 dataset. Individual data points (red) show the actual error values for each speedline.

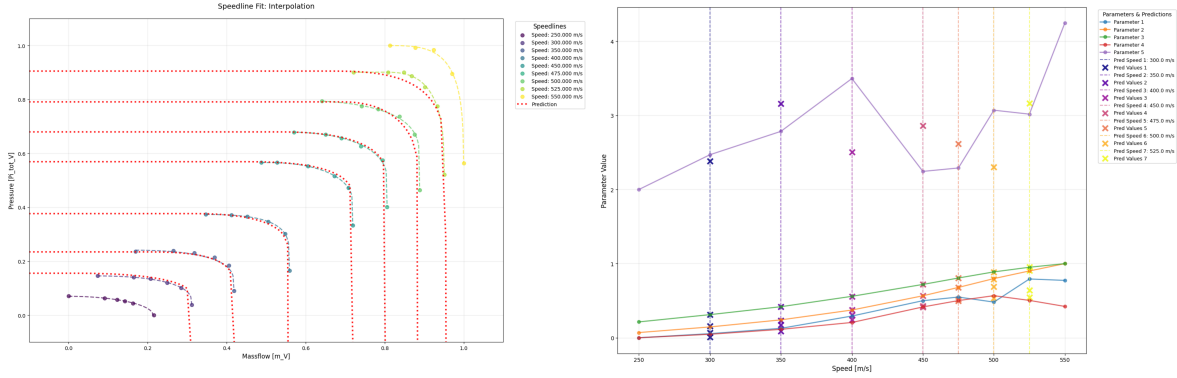


Figure 3: Interpolation results for tca88 compressor. Left: Visualization of predicted speedlines (dashed) compared to actual data (solid) for speeds within the training range. Right: Evolution of model coefficients (β vectors) across different speeds, showing the polynomial interpolation used for prediction.

diction can be attributed to the orthogonal distance being more sensitive to small deviations in regions where the speedline has high curvature, particularly near the choke and surge points. The RMSE of 0.0165 ± 0.0005 for this case better reflects the actual prediction quality we observe visually. The RMSE generally aligns well with visual assessment, with most predictions achieving values below 0.06. Two notable exceptions occur for speed at 400 m/s with $\text{RMSE} = 0.6456 \pm 0.9319$ and speed at 500 m/s with $\text{RMSE} = 1.1437 \pm 2.9239$

These higher RMSE values occur at speeds where the speedline shape changes more dramatically, making the interpolation more challenging. However, as seen in the left plot of Figure 3, even these predictions capture the general trend of the speedline behavior. Table 1 provides a comprehensive overview of all prediction metrics for each speedline.

5.3 Extrapolation beyond CPMs

The extrapolation of speedlines beyond the range of available training data presents significantly greater challenges compared to interpolation. Despite the seemingly logical progression of the β coefficients across speeds (as shown in the right plot of Figure 4), the prediction quality deteriorates substantially when attempting to predict speedlines at the boundaries of the compressor map.

Table 2 presents the complete metrics for the extrapolation predictions. The most striking example is the prediction at 250 m/s (Index 0), where we observe catastrophically high error metrics: $\text{ortho} = 48194.0615 \pm 41051.4939$ and an astronomical MAPE of over 1,000,000%. This extreme deviation clearly indicates that the polynomial interpolation approach, while effective for interpolation, fails to capture the physical behavior of the compressor at lower speeds. The prediction at 550 m/s (Index 8) performs relatively better but still shows considerable error with $\text{RMSE} = 0.6387 \pm 0.8107$ and $\text{ortho} = 1.4420 \pm 2.0146$.

While mathematically sound, the polynomial interpolation of β coefficients appears unable to capture the underlying physical relationships governing compressor behavior at extreme speeds. The model shows asymmetric reliability in extrapolation, with significantly worse performance at lower speeds (250 m/s) compared to higher speeds (550 m/s). In addition to these findings, the smooth progression of β coefficients proves to be a potentially misleading indicator of prediction quality, highlighting the critical importance of thorough validation for extrapolation results.

These results strongly suggest that alternative approaches should be considered for extrapolation tasks. While the current method excels at interpolation within the measured speed range, its limitations become evident when pushed beyond these boundaries. This finding has important implications for compressor map modeling and suggests that physics-informed constraints or different mathematical models might be necessary for reliable extrapolation.

5.4 Performance on the Industrial Dataset

In this section we evaluate our approach on the complete industrial dataset comprising two turbocharger types and 15 CPMs. Again, we distinguish between interpolation and extrapolation. Overall, interpolation delivers promising visual fidelity, whereas extrapolation is unreliable. Error metrics are only partially informative due to extreme outliers and metric-specific pathologies (especially MAPE), so we complement quantitative results with visual inspection.

5.4.1 Reliability of Metrics and Effect of Outliers

A few catastrophic cases inflate averages by several orders of magnitude, especially for Type-1 maps. Means should therefore be interpreted with caution. Robust summaries (medians, trimmed means) would give a more balanced

Table 1: Metrics for speedline predictions (interpolation) on the TCA88 dataset. Each metric is shown with its standard deviation.

Index	Speed [m/s]	RMSE	MAPE [%]	ORTHO
1	300.00	0.06 ± 0.01	64.51 ± 129.75	0.01 ± 0.01
2	350.00	0.02 ± 0.00	9.44 ± 13.97	2.07 ± 4.01
3	400.00	0.65 ± 0.93	161.23 ± 356.93	0.42 ± 0.93
4	450.00	0.05 ± 0.01	7.38 ± 13.64	0.00 ± 0.01
5	475.00	0.04 ± 0.00	3.98 ± 7.74	0.00 ± 0.00
6	500.00	1.14 ± 2.92	102.37 ± 224.04	2.40 ± 3.41
7	525.00	0.06 ± 0.01	5.80 ± 9.02	0.01 ± 0.01

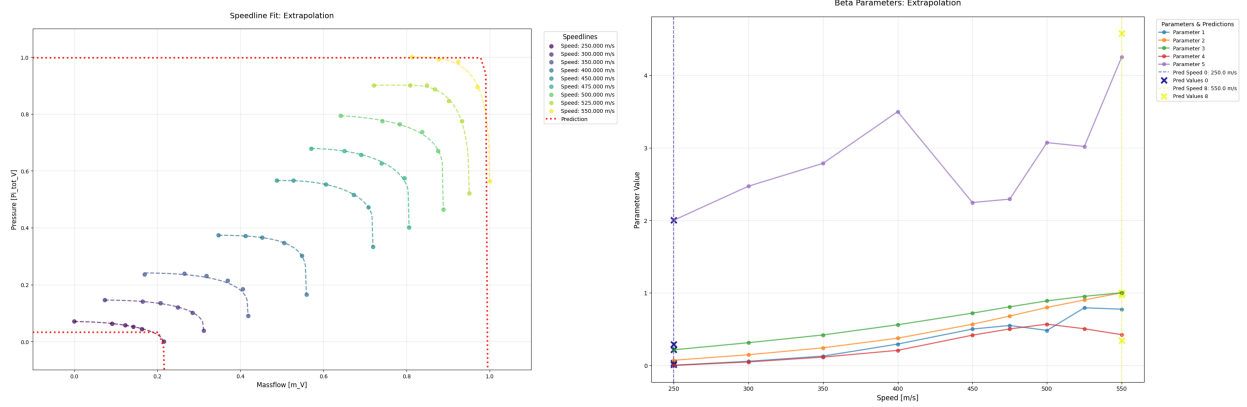

 Figure 4: Extrapolation results for TCA88 compressor. Left: Visualization of predicted speedlines (dashed) compared to actual data (solid) for speeds outside the training range. Right: Evolution of model coefficients (β vectors) across different speeds, showing the polynomial interpolation used for prediction.

Table 2: Metrics for speedline predictions (extrapolation) on the TCA88 dataset. Each metric is shown with its standard deviation.

Index	Speed [m/s]	RMSE	MAPE [%]	ORTHO
0	250.00	0.04 ± 0.00	$1.02e6 \pm 2.27e6$	$4.82e4 \pm 4.11e4$
8	550.00	0.64 ± 0.81	53.31 ± 99.90	1.44 ± 2.01

view. This indicates that outliers dominate means. Regarding the sensitivity of the metrics, we observed that MAPE becomes unstable when denominators approach zero in normalized data, resulting in deceptively large values despite good visual alignment. `ortho` captures geometric fidelity well but can spike near high-curvature regions (surge/choke) even when overall fit looks acceptable. RMSE often aligns best with visual impression but is still affected by local shape changes.

The very high Type-1 averages are caused by a handful of extreme failures. Many Type-1 predictions nonetheless look visually plausible, as summarized in Table 3.

5.4.2 Industrial Dataset: Interpolation

Interpolation works well across most CPMs of the industrial dataset. Despite occasional metric spikes, predicted speedlines usually track the ground truth closely, especially in mid-speed regions. Lower speedlines perform worse than higher speedlines. Predictions are more reliable for CPMs with more speedlines and more measurement points.

We observed three typical situations across CPMs. Results can be visually solid, although metrics are relatively poor due to extreme outliers in specific indices. This is precisely where pure numeric results become misleading: the plot shows the predicted curve adhering to the measured shape for large portions of the speedline. Sometimes situations with very accurate interpolation results, with the predicted speedline closely following the measured curve across the entire range, can occur. Both visual inspection and error metrics confirm high fidelity, highlighting the robustness of the superellipse fitting in well-constrained mid-speed regions. Finally, interpolation can be very poor, especially for low-speed lines with fewer measurement points.

Visual inspection exemplifies the divergence between raw metrics and perceived geometric fidelity. It demonstrates that visually satisfactory predictions can co-exist with discouraging metrics, underlining the importance of qualitative assessment. CPMs can be acceptable in shape despite large reported errors, e.g., if isolated poor indices but an overall reasonable fit occurs.

5.4.3 Industrial Dataset: Extrapolation

Extrapolation (first/last speedlines) is also on the industrial dataset substantially less reliable. Error distributions are heavy-tailed with catastrophic outliers (e.g., type-0 and type-1 boundary indices), indicating that polynomial β -interpolation is not physics-grounded enough at the borders. Visuals often show meaningful trends, but quantitative errors remain high. For industrial application, we recommend restricting to interpolation unless additional physics-based constraints or alternative models are introduced for boundary behavior.

6 Discussion

The results of the fitting optimization study clearly demonstrate that the combination of the `LlamasEllipse` model, DE initialization, Nelder–Mead local solver, and the orthogonal distance metric provides the most reliable and consistent results across different datasets. Each of these elements contributes a specific advantage: The `LlamasEllipse` model inherently captures the geometric characteristics of compressor speedlines more effectively than the `DirectEllipse` approach. While `DirectEllipse` minimizes algebraic error, it often struggles to represent the curved structure of real speedlines, especially near surge and choke regions. In contrast, the `LlamasEllipse` formulation directly parameterizes physically meaningful points, resulting in better fidelity and interpretability.

The optimization process benefits greatly from global search strategies. DE proved particularly effective at providing robust initial guesses, avoiding local minima that hindered the performance of direct or PSO-based initialization. The stochastic population-based nature of DE offers a more thorough exploration of the parameter space, which is crucial given the non-convexity of the fitting problem. For local convergence, Nelder–Mead outperformed L-BFGS-B in difficult cases. While L-BFGS-B is efficient for smooth, well-conditioned landscapes, it can fail in the presence of irregularities or poorly scaled gradients, both common in compressor data. Nelder–Mead, being derivative-free, converged more robustly and provided stable final fits, especially when combined with high-quality DE initialization. The orthogonal distance metric emerged as the most suitable objective function. Unlike MSE, RMSE, or MAPE, `ortho` evaluates the geometric distance between fitted and measured points, aligning directly with the physical goal of reproducing the overall shape of the speedline. Its robustness against outliers and its avoidance of division-by-zero issues make it a stable and interpretable choice. Taken together, these choices explain why the selected configuration (`LlamasEllipse` + DE + Nelder–Mead + `ortho`) yielded the most robust performance in the fitting study. It combines physical interpretability, robust global exploration, stable local refinement, and a geometrically meaningful error metric.

When moving from fitting to prediction, the results show a clear asymmetry between interpolation and extrapolation. Interpolation within the measured speed range works reliably: predicted speedlines generally follow the measured curves closely, with low RMSE and `ortho` values, particularly in mid-speed regions where β -vectors evolve smoothly. This indicates that polynomial interpolation of β -parameters is a valid strategy as long as the target speed lies within the convex hull of the known data.

By contrast, extrapolation beyond the available range proved unreliable. Although β -vectors show a smooth progression across speeds, polynomial models fail to capture the true physical behavior at the boundaries of com-

Table 3: Summary statistics comparing interpolation and extrapolation performance across both compressor types. Note the dramatic increase in error metrics highlighting the method’s limitations beyond the training range.

Metric	Type-0 (Interp.)	Type-1 (Interp.)	Type-0 (Extrap.)	Type-1 (Extrap.)
Number of CPMs	6	9	6	9
Total predictions	37	38	12	18
Average RMSE	0.69	30.15	2.12e3	41.85
Average MAPE [%]	94.27	2.53e4	7.10e10	5.85e8
Average ORTHO	4.23	3.16e4	5.26e8	3.63e8

pressor maps. This is particularly evident at lower speeds, where catastrophic errors occur despite apparently plausible β -trajectories. The mismatch highlights a key limitation: polynomial extrapolation is mathematically consistent but not physics-grounded. It can therefore produce misleading predictions if not carefully validated. While the presented approach demonstrates strong interpolation capabilities and robust fitting performance, several important limitations remain. The most evident limitation lies in the poor extrapolation performance. Polynomial interpolation of β -vectors, while effective within the measured speed range, fails to generalize beyond the boundaries of the compressor map. At low speeds in particular, predictions diverge drastically despite smooth coefficient trajectories. This underscores the fact that polynomial regression, being purely mathematical, does not encode the underlying physics of compressor behavior. Comparable findings have been reported by Shen et al. (2019), who also noted that low-degree polynomials provide satisfactory interpolation but are unreliable for extrapolation.

Sparse data reduces the constraints available for β -vector fitting and weakens polynomial stability, as observed in maps such as CPM (0,4). This limitation aligns with observations in previous work by Llamas and Eriksson (2017), where higher data density was identified as a key enabler for stable parameterization. Although ortho provides a geometrically meaningful measure, it can overemphasize local deviations at surge and choke points, leading to seemingly poor numerical scores despite visually convincing fits. Conversely, MAPE often inflates errors near small denominators in normalized data. This suggests that relying on a single metric is insufficient. A combination of RMSE, ortho, and visual inspection should be maintained for comprehensive evaluation.

Several opportunities exist to improve prediction quality and extend applicability. Incorporating physical constraints (e.g., monotonic behavior near surge, bounds derived from thermodynamic limits) could guide extrapolation and prevent catastrophic divergence. Hybrid strategies that combine polynomial regression with physics-based boundary conditions represent a promising direction. Instead of polynomial regression, spline interpolation or rational functions could provide more stable coefficient evolution across speeds, reducing oscillations and improving extrapolation robustness. Shen et al. (2019) employed quadratic fits; however, more flexible functions may strike a better balance between bias and variance.

A natural extension is the combination of interpretable β -vector parameterization with machine learning methods. Neural networks or Gaussian processes could be trained to map rotational speed to β -vectors, offering data-driven flexibility while retaining a physics-informed representation. This would bridge the gap between purely physics-based and purely data-driven methods, similar to the RNN-based approach of Schulz et al. (2025).

In summary, while the proposed method achieves reliable interpolation with minimal data requirements, it remains limited at the edges of the compressor map and under sparse conditions. Future work should address extrapolation through physics-informed constraints, alternative function families, and hybrid ML integration. Such extensions could eventually enable robust reconstruction of entire CPMs, aligning with the long-term vision of data-efficient, interpretable compressor modeling.

References

- C G Broyden. The Convergence of a Class of Double-Rank Minimization Algorithms. *Journal of the Institute of Mathematics and Its Applications*, 6:76–90, 1970.
- Andrew Fitzgibbon, Maurizio Pilu, and Robert B. Fisher. Direct least squares fitting of ellipses. *IEEE Transactions on Pattern Analysis and Machine Intelligence*, 21(5):476–480, 1999. doi: 10.1109/34.765658.
- Rob J. Hyndman and Anne B. Koehler. Another look at measures of forecast accuracy. *International Journal of Forecasting*, 22(4):679–688, 2006. doi: 10.1016/j.ijforecast.2006.03.001.
- J Kennedy and R Eberhart. Particle Swarm Optimization. In *Proceedings of the Fourth IEEE International Conference on Neural Networks*, pages 1942–1948, Piscataway NJ, 1995. IEEE.
- Oskar Leufvén and Lars Eriksson. A surge-and-choke capable compressor flow model – validation and extrapolation capability. *Control Engineering Practice*, 21(12):1871–1883, 2013. doi: 10.1016/j.conengprac.2013.07.005.
- Xavier Llamas and Lars Eriksson. Parameterizing compact and extensible compressor models using orthogonal distance minimization. *Journal of Engineering for*

Gas Turbines and Power, 139(1):012601–1–012601–10, 2017. doi: 10.1115/1.4034152.

Xavier Llamas and Lars Eriksson. Control-oriented modeling of two-stroke diesel engines with exhaust gas recirculation for marine applications. *Proceedings of the Institution of Mechanical Engineers, Part M: Journal of Engineering for the Maritime Environment*, 233(2): 551–574, 2019.

J. A. Nelder and R. Mead. A Simplex Method for Function Minimization. *The Computer Journal*, 7(4):308–313, 01 1965. ISSN 0010-4620. doi: 10.1093/comjnl/7.4.308. URL <https://doi.org/10.1093/comjnl/7.4.308>.

R. Schulz et al. Automated prediction of compressor performance maps:surrogate-based optimization with rnns for enhanced extrapolation and interpolation. *arXiv preprint arXiv:2506.12345*, 2025.

Haosheng Shen, Chuan Zhang, Jundong Zhang, Baicheng Yang, and Baozhu Jia. Applicable and comparative research of compressor mass flow rate and isentropic efficiency empirical models to marine large-scale compressor. *Energies*, 12(24):4749, 2019. doi: 10.3390/en13010047. URL <https://www.mdpi.com/1996-1073/13/1/4749>.

Rainer Storn and Kenneth Price. Differential evolution — a simple and efficient heuristic for global optimization over continuous spaces. *Journal of Global Optimization*, 11(4):341–359, 1997.